AUT Journal of Civil Engineering

AUT J. Civil Eng., 6(2) (2022) 221-240
DOI: 10.22060/ajce.2022.21183.5796

The durability of Self-Consolidating Concrete Containing Steel Fiber and Two Different Types of Aggregates under the Uniaxial Compression Loading

K. Samimi [1]*, A. A. Shirzadi Javid [2]

[1] Faculty of Civil, Water and Environmental Engineering, Shahid Beheshti University, Tehran, Iran.
[2] School of Civil Engineering, Iran University of Science and Technology, Tehran, Iran.

ABSTRACT: The present study's focus is to investigate the influence of loading micro-cracks on the transport properties of self-consolidating concrete (SCC). To have concrete mixtures with distinctly different fracture properties and diffuse damage behaviors, three SCCs were prepared: two SCCs with two different types of aggregates (limestone and siliceous) and one containing steel fibers. The loading micro-cracks were done on the specimens via the application of uniaxial compression up to 70% of the ultimate compressive strength (UCS) with different loading times to propagate damage within mixtures. Accelerated carbonation was applied to undamaged and damaged specimens with a concentration of CO2 of 20% at 20±5°C and humidity at 70±5% in the carbonation chamber to evaluate the transport properties of SCC. The chloride resistance of the SCC was measured using an accelerated chloride migration test. Based on the results, it was concluded that the transport properties in concrete are highly affected by sustained loading time. The SCC-containing steel fibers showed good resistance against diffusion of chloride ions and CO2 gas for two damaged and undamaged state conditions. Also, a correlation was obtained between the intrinsic permeability coefficient and chloride diffusion coefficient in the damaged and undamaged state for each SCC and also between mechanical damages and durability parameters.

Review History:

Received: Mar. 04, 2022
Revised: Nov. 11, 2022
Accepted: Dec. 12, 2022
Available Online: Dec. 20, 2022

Keywords:

Permeability
Carbonation
Steel fiber
Durability
Self-consolidating concrete

1- Introduction

Cementitious composites are one of the most widely taken materials in the world, and the usage of concrete continues to grow in construction projects [1-4]. Self-consolidating concrete (SCC) is a new concrete that was developed in Japan in the 1980s. SCC development aimed to propose new concrete capable of flowing freely through concrete forms with congested reinforcement. Seismically active regions require significant reinforcement, and it is arduous to vibrate conventional concrete into such forms. An increased amount of cementitious material is needed to achieve SCC properties in cementitious composites [1, 2]. Nowadays, verification of the durability of cementitious mixtures is an essential issue for preventing concrete degradation concerning aggressive agents in the environment [5-7].

Concrete can be defined as multi-phase composites made up of three phases; mortar, mortar/aggregate interface, and coarse aggregate phase. Crack growth in cementitious composites occurs mainly in the cement paste or the aggregate/cement paste interfacial zone. The strength of concrete at the interfacial zone essentially depends on the cement paste's integrity and the coarse aggregate's nature. The formation and propagation of cracks in concrete structures influence their durability. These micro- and macro-cracks created in cementitious composites increase the transport properties. Also, concrete structures deteriorate in their operating environment under harsh environmental conditions and external loading. Although the performed load can lead to specific degradation of the structure, the primary long-time deterioration mechanism involves moisture penetration and the transport of chlorides within concrete. The gas permeability of concrete, its resistance to chloride ingress, and carbonation by diffusion of CO_2 gas are usually considered critical properties for reinforced concrete's durability [8, 9]. Concrete structures used in marine structures generally suffer from the coupled attack of chloride diffusion and scouring. To build durable and reliable structures, accurately predict the penetration of moisture and chlorides within concrete.

The behavior of concrete structures in high-intensity stress conditions must be investigated to ensure the safety of public buildings. Aggregates manufacture a significant part of the volume of concrete. This shows that the presence of aggregates most likely influences concrete properties. More recently, the effect of the shape and nature of coarse aggregates on cementitious composite's triaxial behavior was studied on three concrete distinguished by the type of coarse aggregates (siliceous, limestone, and glass) [10, 11]. It has been observed that coarse aggregates' nature controls concrete's volumetric behavior in high confinement. However, this only slightly affects the deviatoric strength of the concrete.

*Corresponding author's email: k_samimi@sbu.ac.ir

Fig. 1. Photo and schema of steel fibers.

The relationship between concrete structures' mechanical and transport properties has been under evaluation over the last few years [12]. Cracks accelerate water penetration and the diffusion of aggressive ions, such as chloride, leading to damage and durability problems [13]. In 2005, Chatzigeorgiou *et al.* [14] evaluated the coupled problem of mechanical damage and the permeability of concrete. They concluded that for low to high-stress levels, the permeability of concrete is drastically increased when the load is very close to the material's ultimate compressive strength (UCS). In specimens subjected to 70% of UCS uniaxial compression, Samaha and Hover [15] showed the existence of micro cracks.

The concrete shows 15 to 20% less fluid and ion penetration in this state. Chloride ion diffusion measurement follows the same behavior for loads up to 80% [12, 16, 17]. or 90% of the peak [18]. Repeating a compression load between 60 and 80% also increases permeability by extension of microcracking. Micro cracks seem interconnected, leading to changes in a cementitious material's transfer properties. Tegguer *et al.* [19]. Investigated the influence of mechanical damage on durability properties such as diffusion and permeability coefficient. The results obtained on the damaged diffusion and permeability show that the transport properties are affected by the damage [20, 21]. In the case of ordinary concrete, the previous studies [16, 19] found an increase in damaged permeability to undamaged permeability ($K_{int}(d)/K_{int}$) by a factor of 10 while that relating to the diffusion coefficient ($D_e(d)/D_e$), increases by a factor of 2.5. For high-performance concrete, the $K_{int}(d)/K_{int}$ ratio increases by a factor of 7, while $D_e(d)/D_e$ increases by a factor of 1.9.

Some recent research [16] found that using steel fibers in concrete has a limited effect on the impact resistance of the materials. The results also indicated that microfibers offer better impact resistance than longer fibers [16].

2- Research Significance

The main focus of this research is to evaluate the impact of produced micro-cracks under loading on transport properties such as gas permeability, chloride diffusivity on steady state, and accelerated carbonation for three SCC mixtures performed by two different types of aggregates and steel fibers at 90 days of aging. Damage in the SCC specimens is characterized by the measurement of the decrease in the elastic modulus. This last is measured using ultrasonic waves apparatus.

3- Experimental Program

3- 1- Materials

Two coarse aggregates (G) of 6.3/10 mm nominal size used in this study were limestone and siliceous gravel with a density of 2.7 and 2.58 t m^{-3} and a water absorption coefficient of 0.7 and 0.48%, respectively. A natural sand (S) of 0.4 mm nominal size with a density of 2.6 t m^{-3} and a water absorption coefficient of 1.2% was used as a fine aggregate. The composites' binder is made using Portland cement with 98% clinker and limestone filler (LF). The fiber lengths were 35 mm, as shown schematically in Fig. 1, and specify the properties in Table 1. A high-range water-reducing admixture (HRWRA) based on chains of modified poly-carboxylate ether was also used. Its density was 1.1 g/cm^3 (at 20 °C), and the PH is 4.8 ± 1.00. The dosage can range from 0.2 to 3% of the binder's or cement's weight, depending on the fluidity and performance required. The superplasticizer dosage is experimentally determined from tests on fresh concrete to obtain a slump flow diameter of 670±20 mm for all SCCs composites.

3- 2- Mixtures proportions

Three SCCs were prepared using the same water-to-binder ratio (W/B) of 0.38 and a constant total binder content of 600 kg/m^3. Table 2 shows the mixtures proportions of the SCCs studied in this research. Two SCCs were made using the limestone aggregates and siliceous aggregates, SCC PC-LA and SCC PC-SA, respectively. Another SCC is reinforced

Table 1. Fibers characteristics.

Fiber type	*Steel*
Length (mm)	35
Diameter (µm)	29
Density (g/cm³)	7.8
Modulus of elasticity (N/mm²)	210000

Table 2. Mixture proportioning of the SCCs. All quantities are in kg/m³ of fresh SCCs.

Composition (kg/m³)	*SCC PC-LA*	*SCC PC-SA*	*SCC PC-LA/F*
Limestone aggregates	810	-	810
siliceous aggregates	-	810	-
Sand 0/4	830	830	830
CEM I 52.5N	400	400	400
Steel fibers (% by volume)	-	-	0.4
Limestone filler	200	200	200
Water	230	230	230
Superplasticizer	2.3	2.1	2.9
w/b	0.38	0.38	0.38

with steel fibers of 0.4% by volume using only the limestone aggregates (SCC PC-LA/F).

3- 3- Testing methods

3- 3- 1- Compressive strength

A compressive strength test is performed on the cylindrical specimen (Φ110 mm x H220 mm). The strength was checked after 7, 28, and 90 days of curing.

3- 3- 2- Water absorption

The porosity accessible to water (ε) is measured on the cylindrical specimen (Φ110 mm x H50 mm) according to NF P 18-459 standard. It is calculated using Eq. (1):

$$\varepsilon = \frac{M_s - M_d}{M_s - M_w} \quad (1)$$

where M_s is the mass of the saturated specimen, is the mass of the dried specimen after thermal treatment at 105°C until stabilization of mass; is the mass of a saturated specimen immersed in water.

3- 3- 3- Mercury intrusion porosimetry (MIP)

The MIP test is widely used to determine the total volume and pore size distribution in the meso- and macro-pore ranges. Two samples for each mix and each loading cycle were carefully cored from the specimens and dried at 40 °C. Various pressure levels were applied from $3x10^{-3}$ to 200 MPa, covering a pore diameter range from 0.003 to 360 µm.

3- 3- 4- Steady-state migration test

This is an accelerated diffusion test by the application of an electric field. The experimental protocol consists of the position of the saturated cylindrical sample by a solution of NaOH between two compartments of the migration cell [22], as shown schematically in Fig. 2. The upstream compartment contains a saline solution (0.5mol NaCl + 0.3mol NaOH, "Cathode"), and the downstream compartment a basic solution (0.3 mol NaOH, "Anode") without chlorides. For each composite mixture, three test specimens (Φ110 mm x H50 mm) were taken from three cylindrical samples (Φ110 mm x H220 mm) that were stored in a climate room at 20 ± 2 °C and R.H > 95 % up to 90 days.

The stainless steel mesh electrodes were connected with a power supply in such a way that the voltage was across the concrete specimen. The potential difference (ΔE) was fixed at 20 V (4V/cm). The value is sufficient to accelerate the movement of chlorides without causing excessive

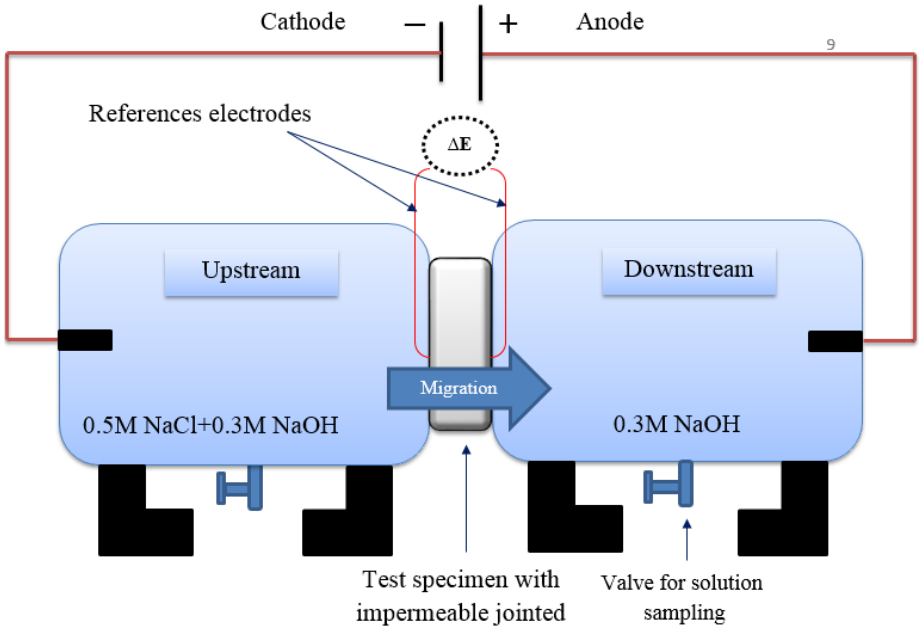

Fig. 2. Schema of migration cell used in this study.

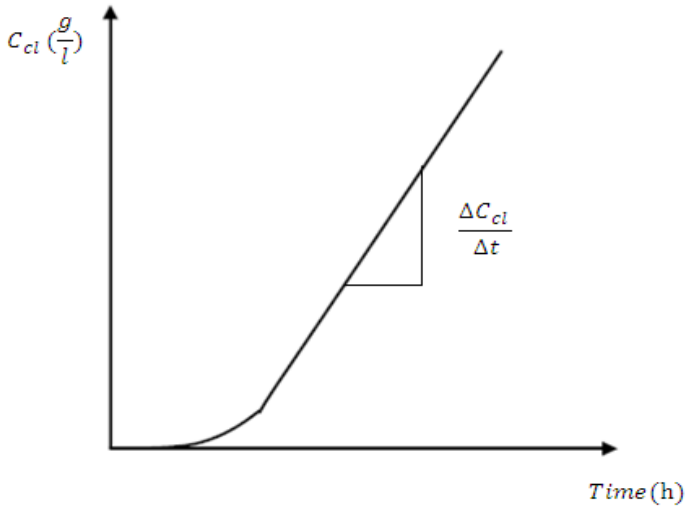

Fig. 3. Schematic variation of the chloride concentration with time in compartment 2.

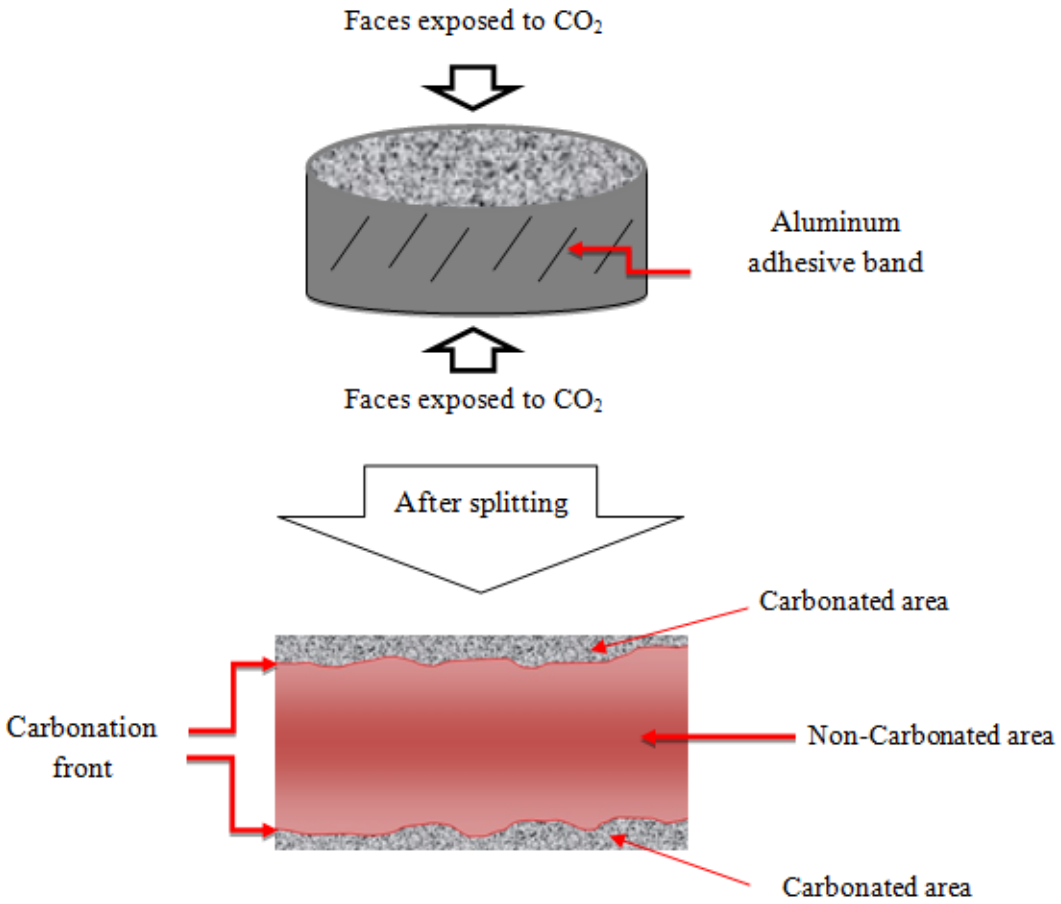

Fig. 4. Position the faces exposed to carbonation and faces protected by an aluminum film.

temperature rises or causing disturbances in the electrodes, especially hypochlorite formation [9]. The chloride migration test under an electric field determines the apparent or effective migration coefficient depending on whether the test is carried out in a Non-steady state or steady-state conditions. During the test, the chloride ion concentration was determined according process described by [23] and Fig. 3.

3- 3- 5- Accelerated carbonation test

The accelerated carbonation test was carried out according to the procedure recommended by the working group and cited in the GranDuBé project, 2007 [24]. The SCCs specimens are cured in an accelerated carbonation chamber with controlled humidity and temperature. The concentration of CO_2 in the chamber was maintained at 20%, the temperature was maintained at 20±5 °C, and humidity was kept at 70±5%. Three cylindrical samples of Φ110 x H50 mm were cut from the central portion of each cylinder SCC (Φ110 x H220 mm) after mechanical damage for the carbonation test. Then they were sealed by an aluminum adhesive band to transfer a unidimensional diffusion of CO_2 through the specimens, as shown schematically in Fig. 4. Concrete samples were kept in an oven at 40 °C for 14 days and then in a carbonation chamber for up to 28 days. When the specimens reached the carbonated age to be tested, the specimens were taken out and split into two half-cylinders along the length. The freshly broken surfaces were sprayed with a color indicator of pH (phenolphthalein) [25].

3- 3- 6- Gas permeability

Apparent permeability was measured using a Cembureau constant head permeameter [26]. Permeability measurements were prepared in an air-conditioned room (20 ± 1 °C and RH 50 ± 2%). Three cylindrical samples of 50 mm thickness were cut from the central portion of each cylinder for testing and placed in a triaxial cell, and injection pressure in these tests was applied below. The setup to perform gas permeability measurements were designed to work as a constant head permeameter under different gas pressures, with the possibility to change the head value and measure the gas inflow and outflow (Fig. 5).

3- 3- 7- Producing micro-cracks by uniaxial compressive loads

After 90 days of hardening, the cylindrical specimens (Φ110 x H220 mm) are loaded by a hydraulic press under uniaxial compression up to 70% of the ultimate compressive strength (UCS) to create internal damage into the test

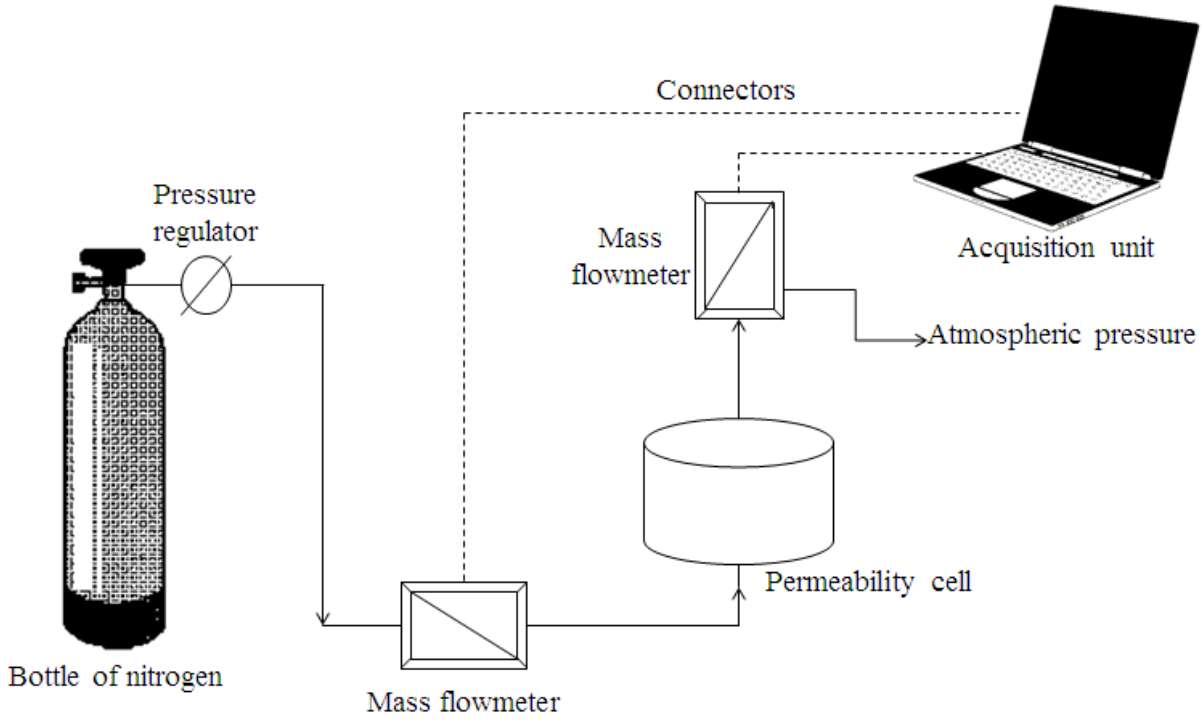

Fig. 5. Schema of experimental device used for measuring the gas permeability.

specimens. The loading times were maintained for 1, 2, and 4h, allowing cracks propagation in cylindrical specimens (see schematically in Fig. 6) [27]. The loading and unloading stress ratio is 0.6 MPa/s.

3- 3- 8- Damage evaluation

Damage is supposed to accumulate inside concrete specimens when loads are applied, leading to micro-cracks. The evaluation of the variation of elasticity modulus is used to calculate the damage variable, which indicates the degree of micro-cracking. A damage parameter *d* in damage mechanics can be defined from the relative ratio of modulus in elasticity [26] by Eq. (2):

$$d = \frac{E_0 - E}{E_0} \quad (2)$$

where E_0 is the initial modulus of elasticity, and E is the final modulus of elasticity obtained for damaged concrete.

To evaluate the amount of damage, i.e., micro-cracks of specimens, the dynamic modulus measurements of the concrete cylinders are carried out immediately before and after loading. The decrease recorded in the dynamic modulus is due to the appearance of micro-cracks inside the material during the loading phase.

4- Results and Discussion

4- 1- Compressive strength

The compressive strength of the SCCs up to 90 days of aging is shown in Fig. 7. As can be expected, all the studied SCCs' compressive strength is enhanced by age. This enhancement is more visible for SCC with fibers. The SCC with the siliceous aggregates shows a lower compressive strength of 11% than the SCC prepared with the limestone aggregates at 90 days of aging. It offers higher resistance by 11 and 13% relative to limestone and siliceous aggregates, respectively, at 90 days of aging, which shows the reinforcement of SCC by steel fibers.

4- 2- Water absorption

Fig. 8 presents the water absorption results for damaged and undamaged conditions up to 4 hours of loading for three studied SCCs at 90 days. As expected, experimental results show increased water porosity with increased loading time for all three studied SCCs. Among the three mixtures, SCC based on steel fibers exhibits lower water absorption values, SCC with limestone aggregates, and SCC with siliceous aggregates. During an hour of loading, the SCCs were about 7–9% more porous than their references (undamaged condition). At two hours of loading, an increase in porosity was observed between 15-19%. SCC with the siliceous aggregates shows a slightly higher porosity increase than two other SCCs during mechanical loading. At four hours of

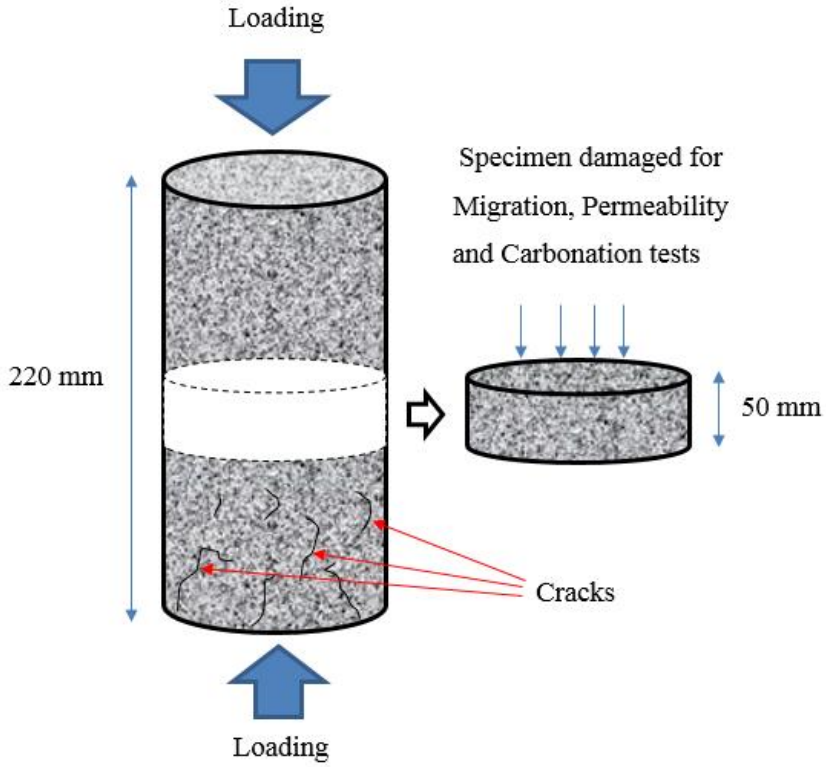

Fig. 6. Schema of the experimental setup for compressive loading test.

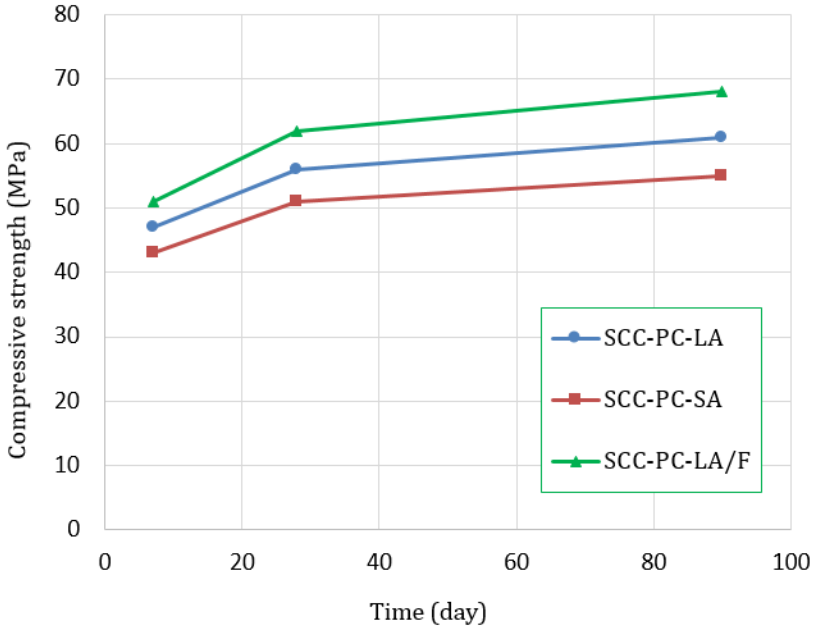

Fig. 7. Evolution of the compressive strength of the studied SCCs with curing time.

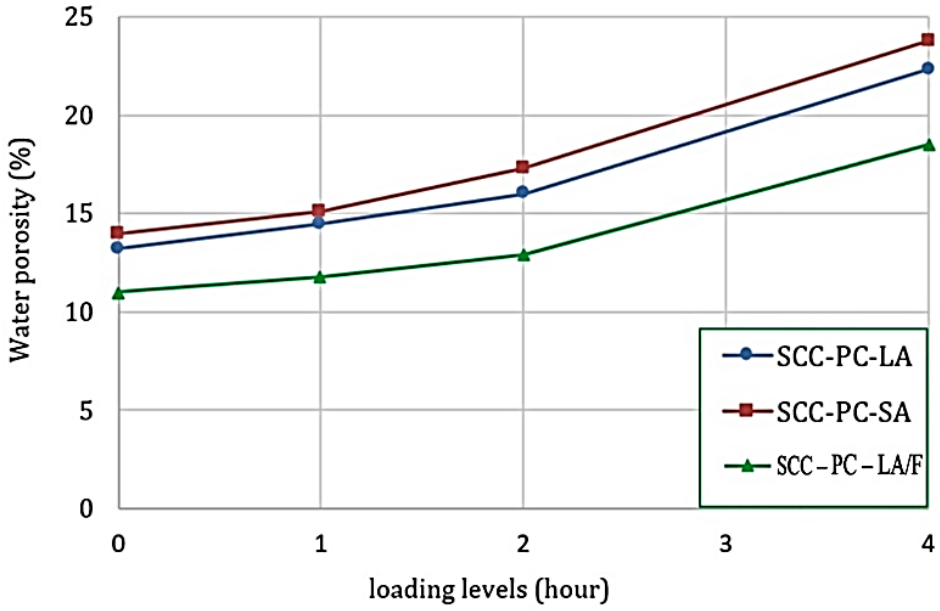

Fig. 8. Water porosity of the studied SCCs at 90 days of aging with different loading states.

Table 3. The diffusion coefficient and penetration time values.

References	*Time of penetration of Cl^-, T_{pass} (h)*	*Migration coefficient (m^2/s)*
SCC-PC-LA	60	2.89×10^{-12}
SCC-PC-SA	42	3.1×10^{-12}
SCC-PC-LA/F	80	2.1×10^{-12}

loading, the higher porosity increase may be attributable to damage between inclusions and the matrix. It is more evident for SCC based on siliceous aggregates due to the presence of an Interfacial Transition Zone (ITZ) between the aggregates and the cement paste, which has a lower resistance than cement paste [28]. The water absorption of the SCC with the steel fibers is lower than the two SCCs without fibers under loading. Thus, including steel fibers can increase strength in the SCC and decrease crack width, which will be effective for concrete durability.

4- 3- Chloride ion migration

The chloride ions are shown in Table 3 and Fig. 9. The results are based on the average obtained from three replicate samples tested for each SCC. The concentration of chloride migration through SCCs shows an exponential relationship called the non-steady-state (chloride ions are penetrating through saturated pores in the specimen and have not reached the anode cell). Then increases with the testing time after a different stage that shows an approximately linear relationship called steady-state (flux of chloride ions passing through the specimen becomes constant).

To compare the resistance of the SCCs based on three kinds of mixtures against the concentration of chloride migration through concrete, the SCC with the steel fibers showed higher resistance to chloride migration by 27% and 32% relative to SCC-PC-LA and SCC-PC-SA, respectively. This decrease in chloride migration for the SCC based on steel fibers may be explained by its lower porosity value and more significant tortuosity compared to SCCs manufactured by limestone and siliceous aggregates.

The time to penetrate Cl^- is more remarkable for the

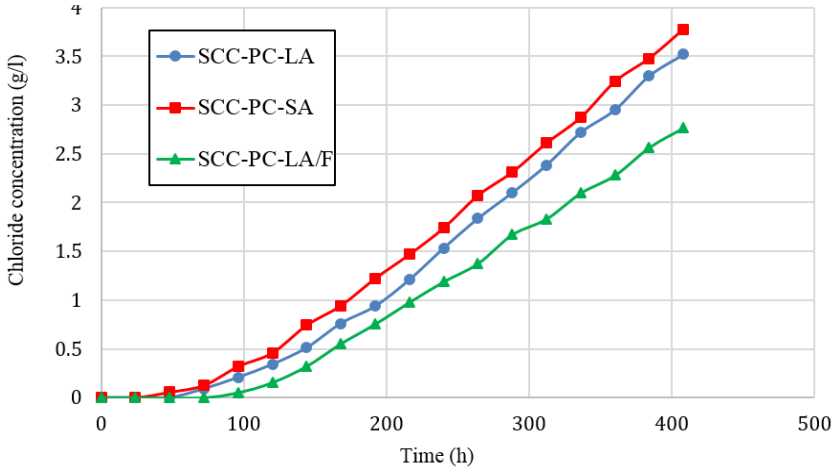

Fig. 9. Evolution cumulative increase of chloride in the downstream cell.

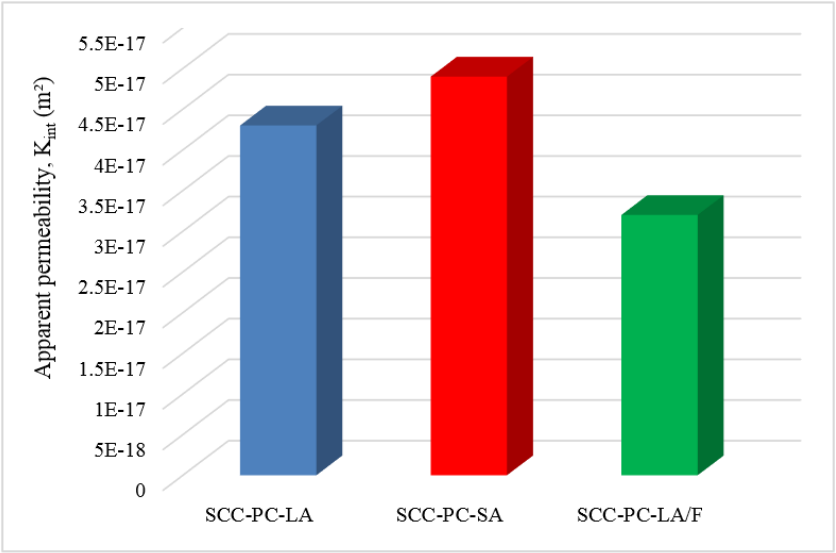

Fig. 10. Evolution of the intrinsic permeability.

SCC based on steel fibers (80h), with a decrease of the diffusion coefficient of 27% and 32% compared to SCCs based on limestone and siliceous aggregates, respectively. It is also observed that a penetration time reduction depends on the aggregates' nature. However, the time of penetration of chloride ions is essential, showing good resistance to the penetration of Cl^{-}.

4- 4- Gas permeability

The results of intrinsic permeability for SCCs are given in Fig. 10. The results show that aggregates influence gas permeability in the SCCs. The results show that the inherent permeability coefficient K_{int} of SCC based on siliceous aggregates is higher than the SCC with the limestone aggregates. It is generally observed that the adding fibers in concrete, a lower intrinsic permeability coefficient is succeeded by 26 and 35% than the SCCs without fibers based on limestone and siliceous aggregates, respectively. The relative permeability was intrinsic of damaged cementitious composites $K_{int}(d)/K_{int}$ is defined as the ratio between the permeability coefficient of damaged cementitious composites $K_{int}(d)$ and the permeability coefficient of undamaged cementitious composites K_{int}. It can be related to the damage variable "d". The increase in permeability relative to

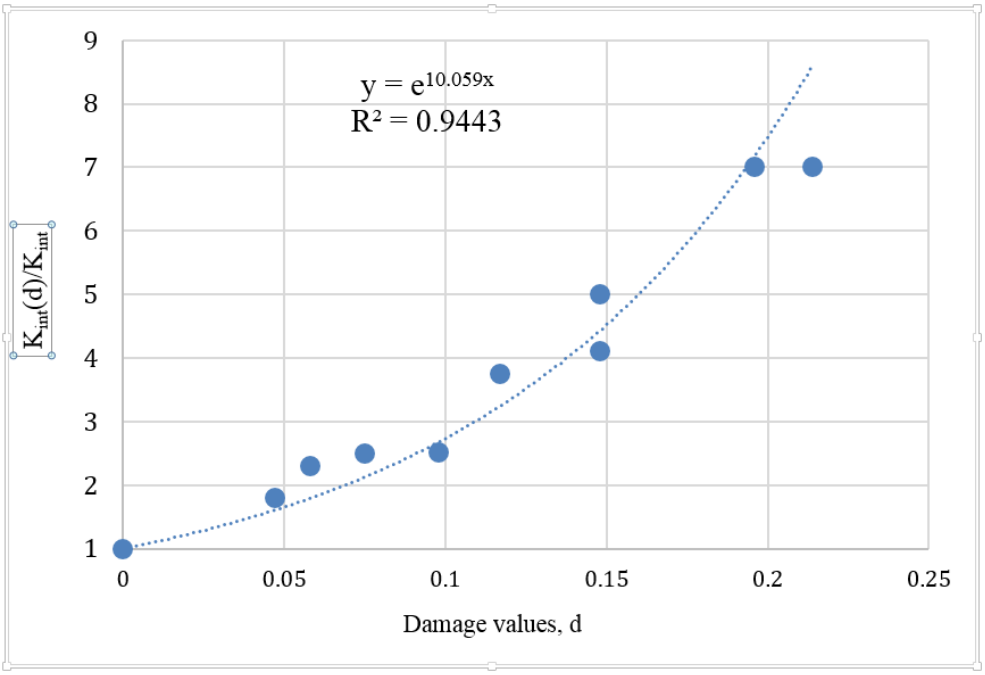

Fig. 11. Relation between the increase in permeability intrinsic and damage value.

permeability $K_{int}(d)/K_{int}$ with the damage coefficient evaluated by the dynamic method is illustrated in Fig. 11. Based on the types of mixtures and duration of the loading state, and the damage values range between 0.047 and 0.214 at 70% of the ultimate compressive strength (UCS). Consequently, the material's elastic modulus gradually decreases, and residual strains appear, leading to material degradation. The damage coefficient (d) evaluated by the dynamic method of SCC composite based on limestone aggregates is lower than the SCC based on siliceous aggregates for the same loading time. This result confirms that the microcracking patterns of the SCC composite based on siliceous aggregates are more significant than that of the SCC composite with the limestone aggregates. $K_{int}(d)/K_{int}$ tended to increase slightly with the damage coefficient of three SCCs composites. This range of damage coefficient corresponds to the observed load level, which was found to be 70% of the ultimate compressive strength (UCS) with a different loading state. An exponential curve for the relative increase of gas permeability was obtained as a function of the damage coefficient. This relation was obtained in the range of $d < 0.214$. A similar relation was obtained by [16, 19, 29] using uniaxial compression tests that the stress levels vary between 60% and 90% of the ultimate strength.

The Klinkenberg coefficient was calculated from the linear slope by measuring apparent permeability at different injection pressures. This coefficient was linked with intrinsic permeability in Fig. 12. The Klinkenberg coefficient increases with the decrease in inherent permeability. This might be explained by the lower network porosity of the SCC fibers composite than the SCCs based on limestone and siliceous aggregates, which show a lower gas permeability for the SCC composite with the fibers. These results are in coherence with the evolution of differential pore size distribution for the SCCs composites obtained from mercury porosity due to loading. Cementitious composites are capillary porous materials whose permeability closely correlates with their microstructure.

4- 5- Mercury Intrusion Porosimetry (MIP)

This section discusses the evolution of differential pore size distribution for the SCCs at undamaged conditions and a 4h loading state. The cumulative intrusion as a function of pore diameter and differential curves is shown in Fig 13. The MIP test data indicate a threshold radius below which there is relatively little intrusion and immediately above where rapid intrusion commences. This corresponds to the region of inflection, following an almost horizontal portion of cumulative intrusion curves. The test results also indicate that the threshold radius increases with increasing loading time. As loading time increases, the threshold region tends to flatten out, and the threshold radius rises progressively. This can be attributed to the micro-cracks effect and reorientation of the pore system into the SCCs. Unlike cementitious composites, the SCC threshold radius is linked to the binder-aggregate interface or fissures rather than to the pores alone [30].

It can be found in Fig. 13 that the character of pore size distribution curves of SCCs is influenced by loading time. Different SCCs have different pore structures depending on the aggregates and steel fibers used. SCC based on siliceous

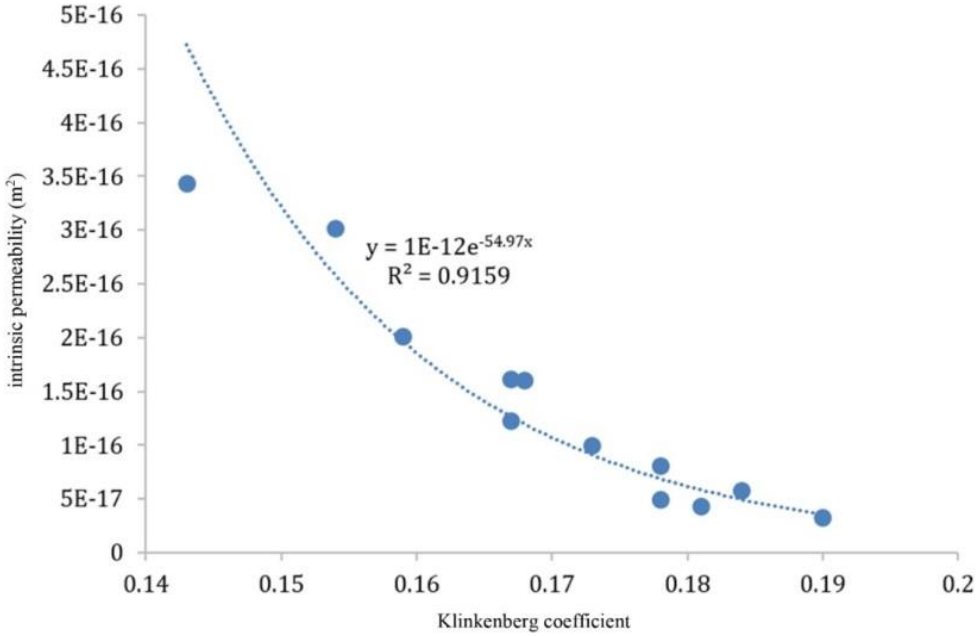

Fig. 12. Evolution of the intrinsic permeability versus Klinkenberg coefficient (β) of SCC composites.

aggregate has a slightly greater pores volume. This is consistent with experimental research from Gonc *et al.* [31]. Differential curves for SCC based on steel fibers exhibit a lower distribution of pore sizes in undamaged conditions. As loading time increases to 4h, another pore family appears at a larger pore size for SCCs, presenting several peaks on their differential curves. These peaks indicate mercury intrusion through a pore network connected to micro-cracks in these concretes [32, 33]. These peaks are more intense for SCC based on siliceous aggregates due to the development of micro-cracks in this SCC with increasing loading time. Concretes' mechanical and transport properties can influence this phenomenon in their lifetime.

4- 6- Effect of uniaxial damage on chloride diffusion

The accumulation of chloride ions in the downstream compartment is shown as a function of time for the damaged and undamaged SCCs composites in Fig. 14.

The results showed that for damaged SCCs composites, the chloride diffusion coefficient increased with the increase of the porosity due to the applied load we showed from the MIP test. The applied load up to 70% of the ultimate compressive strength (UCS) for 1, 2, and 4h, the relative diffusion coefficient of damaged to undamaged concrete (De(d)/De) are higher for the SCCs composites based on siliceous aggregates than two others SCCs composites. The average diffusion coefficients for the damaged specimen De(d), from the flux of chlorides passing to the downstream compartment, are given in Table 4. The results show that for damaged SCCs composites, is higher than for undamaged SCCs composites. A lower T_{pass} may result from a higher porosity. This is an effect of the applied load, which increases the porosity. T_{pass} depends on the porosity of concrete and chloride binding [34, 35]. However, for damaged specimens, it appears that T_{pass} decreased with the diffusion coefficient De increasing due to the presence of microcracks in cementitious composites. Fig. 15 compares the diffusion coefficient of damaged to undamaged cementitious composites ($D_e(d)/D_e$) at 1, 2, and 4h of loading for SCCs composites. According to the results, composites based on siliceous and limestone aggregates show the same increase in (De(d)/De) with increasing loading time and a better ratio over the entire loading time.

Nevertheless, SCC composites with fibers are characterized by some micro-cracks developing over time, followed by a rise in pore volume due to loading. The relative diffusivity of damaged cementitious composites $D_e(d)/D_e$ is defined as the ratio between the diffusion coefficient of damaged cementitious composites $D_e(d)$ and the diffusion coefficient of undamaged cementitious composites D_e. It can be related to the damage variable "d". Fig. 16 presents the evolution of relative diffusivity of damaged cementitious composites with damage value assessed by the dynamic method. The relative diffusivity of the SCC composite with the fibers for the load level of 70% of UCS is lower than the SCCs composites based on limestone and siliceous aggregates for all of the loading states. From Fig. 17, the relationship between these two parameters can be expressed by a linear function with a correlation coefficient $R^2 = 0.93$. This linear function is similar to that obtained for gas permeability with different empirical coefficients. This allows for an empirical

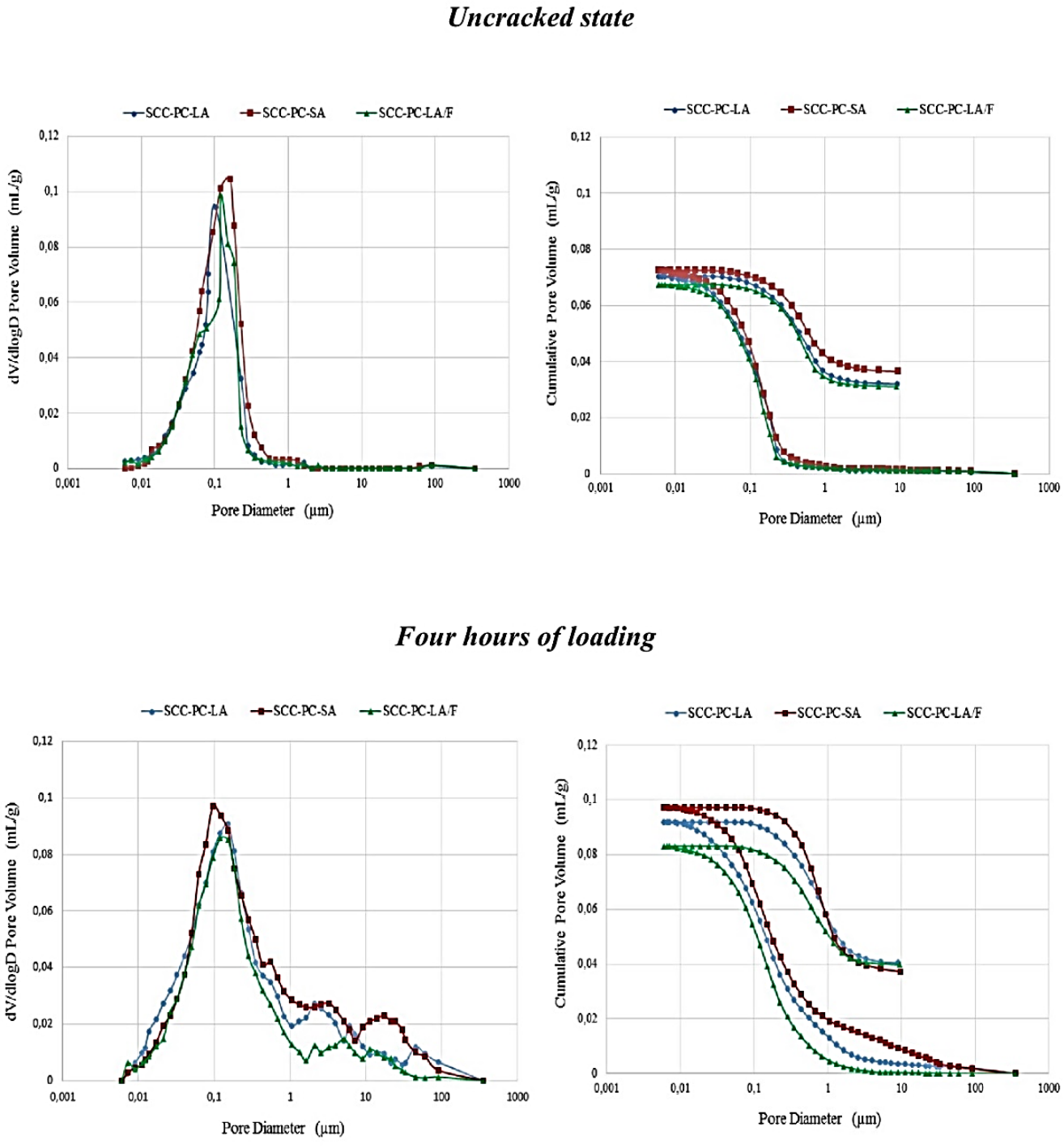

Fig. 13. Differential pore size distribution of SCCs as a function of loading state.

Table 4.The diffusion coefficient and penetration time values for the damaged SCCs.

Mixtures	*1 hour*		*2 hours*		*4 hours*	
	$D_e \times 10^{-12}$ (m²/s)	T (h)	$D_e \times 10^{-12}$ (m²/s)	T (h)	$D_e \times 10^{-12}$ (m²/s)	T (h)
SCC-PC-LA	3.41	32	4.34	24	6.73	12
SCC-PC-SA	3.69	24	4.65	18	7.5	12
SCC-PC-LA/F	2.26	40	3	36	4.5	24

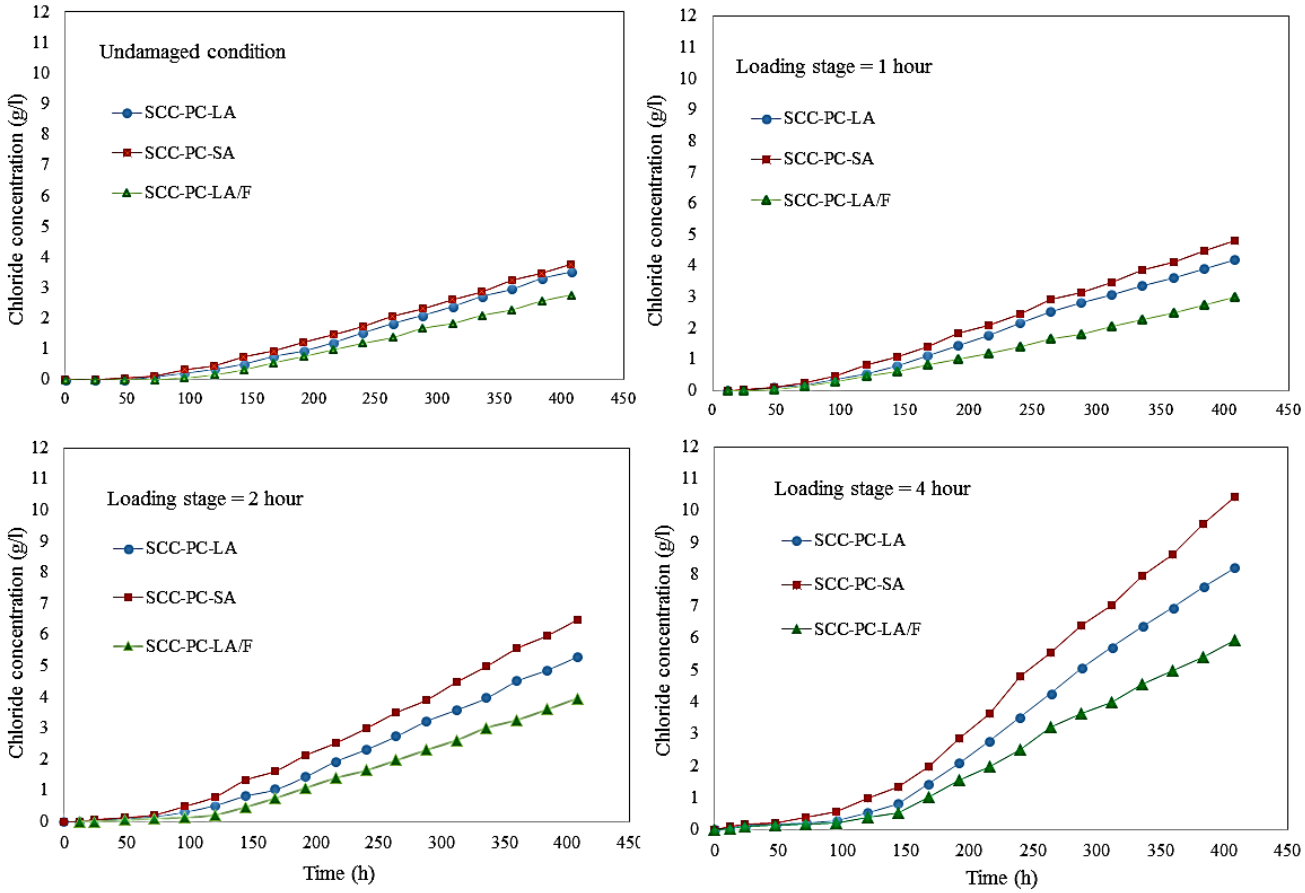

Fig. 14. Evolution cumulative chloride increase in a downstream cell for the undamaged and damaged SCC composites.

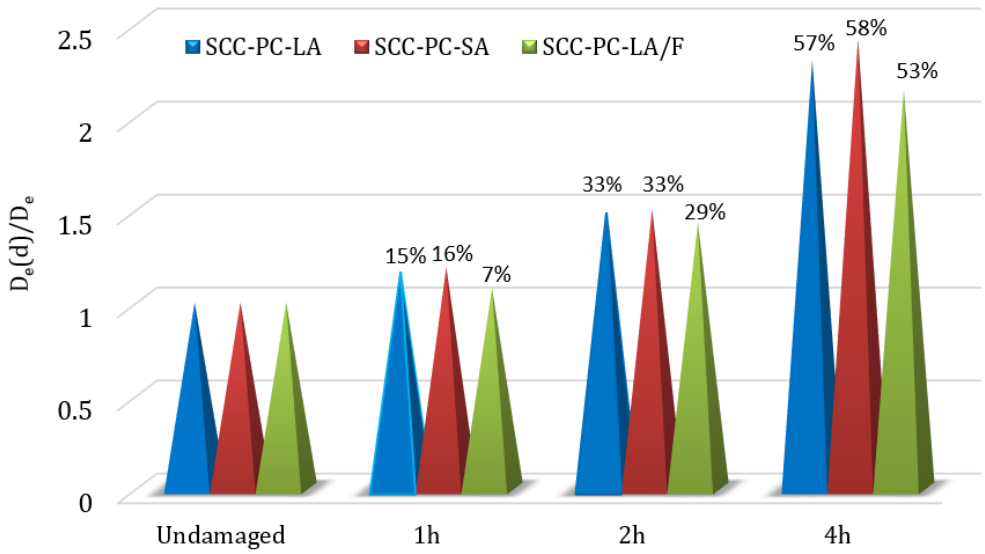

Fig. 15. Comparison of the diffusion coefficient of damaged to undamaged concrete (De(d)/De) at 1, 2, and 4h of loading for SCC composites.

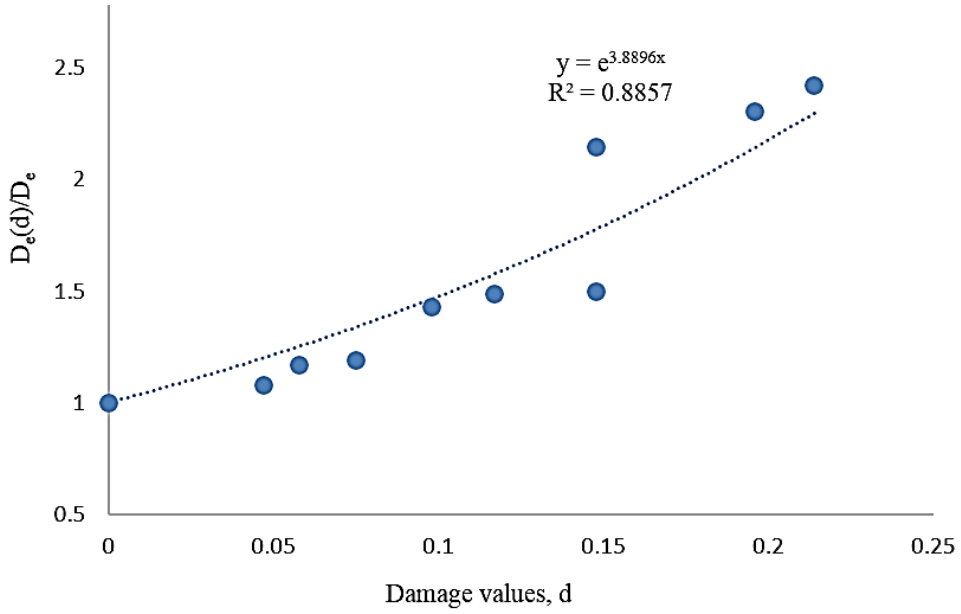

Fig. 16. Relationship between increased chloride diffusion coefficient and damage value.

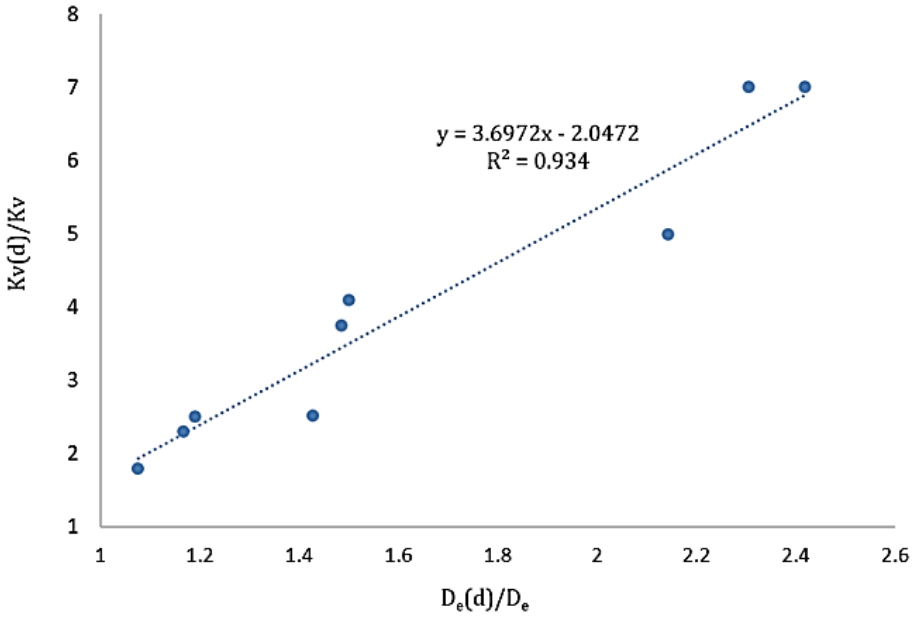

Fig. 17. Relationship between increasing the gas permeability and chloride diffusion coefficient.

relationship between these transfer parameters, even if they do not correspond to the same transport mechanisms.

Two transport modes govern gas permeability and diffusivity. Both parameters vary depending on the microstructure of cementitious composites and the degree of cracking that is indicated by damage. According to the equations presented in Figs.11 and 16, it is found that the gas permeability and diffusion coefficient show the same trend based on the damage variable. This allows us to establish a relationship between these two transfer parameters. Gas permeability is measured on a dry sample as the diffusion coefficient is calculated on the sample in the saturated state by migration test under steady-state conditions. Fig. 18 shows a linear variation of $K_{int}(d)/K_{int}$ with the ratio De(d)/De for SCCs composites depending on the damage variable, specific for each composite type.

The existence of a microcrack network seems to modify the sustainability indicators significantly. However, the influence is different for each composite. It is observed that gas permeability is more sensitive to damage: in the case of SCC composite based on siliceous and limestone aggregates, $K_{int}(d)/K_{int}$ increases by a factor of 7 for both while De(d)/De increases by a factor of 2.42 and 2.3, respectively.

This tendency was already observed previously; the gas permeability changes significantly with the increase of damage level [19, 36, 37], while chloride penetration is much less affected by cracks [19, 38]. This result confirms that microcracking obtained with uniaxial compressive loading impacts the transfer parameters for cementitious composites with high porosity. It is noted that the relative permeability increases linearly with the relative diffusion coefficient.

4- 7- Effect of uniaxial damage on accelerated carbonation

Fig. 18 shows the relationship between loading time from uniaxial compressive and carbonation depth at 28 days of curing in an accelerated carbonation chamber. For the SCCs composites, the carbonation depth of damaged specimens was deeper when compared to the unstressed specimens. Furthermore, the carbonation depth constantly increased with an increase in loading time. However, the rate of growth is different for the SCCs composites specimens. The carbonation rate of SCC composite based on siliceous aggregates was faster than that of SCC composite with limestone aggregates and SCC fiber composite. The difference between the carbonation depths of these SCCs composites increased with loading time. At 28 days, when the loading time was increased from an hour to four hours, the difference increased from 6.7 to 18.5 mm for SCC-based siliceous aggregates, from 5.3 to 15.5 mm for SCC-based limestone aggregates and from 3.9 to 11.5 mm for SCC composite with the fiber as shown in Fig. 18. Many pores exist in concrete structures because of cementitious composites' nature. Cementitious composite microstructures contain numerous visible and invisible cracks resulting from shrinkage and external loads. Generally, cracks in cementitious composites change the discontinuous material into a continuous one when they connect the internal pores. Due to such continuities, CO_2 in the environment can easily penetrate cementitious composites' interiors and accelerate

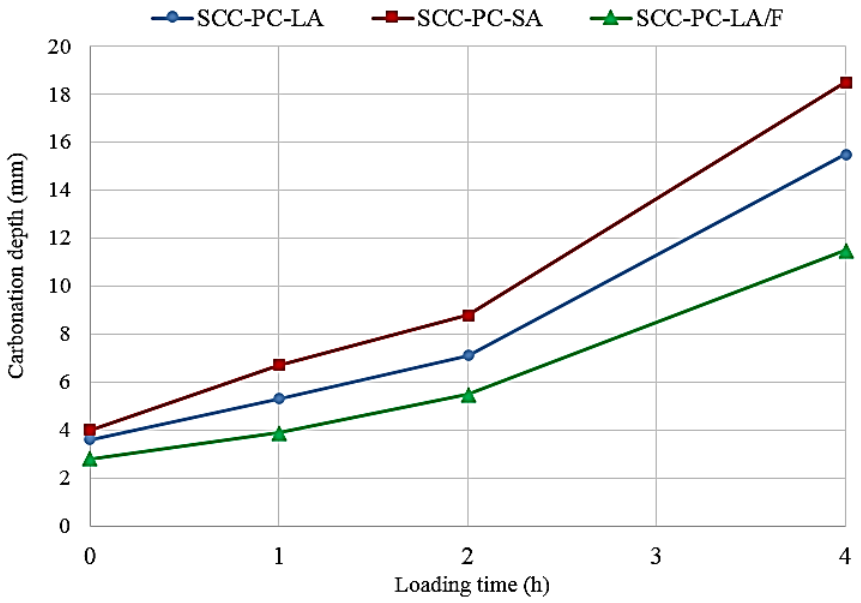

Fig. 18. Evolution of carbonation depth of three SCC composites as a function of loading time.

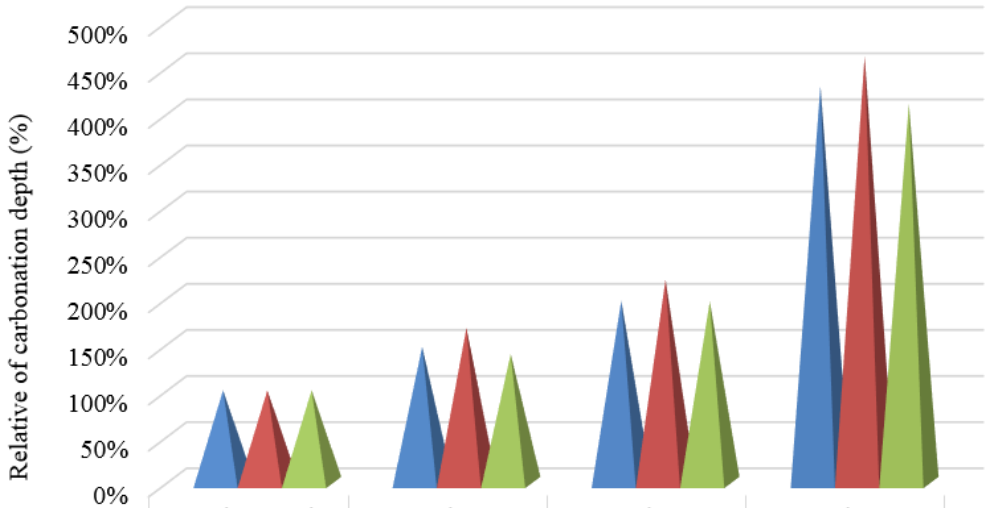

	Undamaged	1h	2h	4h
SCC-PC-LA	100.00%	147.22%	197.22%	430.56%
SCC-PC-SA	100.00%	167.50%	220.00%	462.50%
SCC-PC-LA/F	100.00%	139.29%	196.43%	410.71%

Fig. 19. Histogram of the relative carbonation depth of SCC composites as a function of the loading time.

the carbonation process. As reported in the literature [39-41], cracks' size, volume, and connectivity directly affect the diffusion rate of CO_2 in cementitious composites. Fig. 19 shows the carbonation depth of three SCCs composites. For the three composites, residual carbonation depth increases with the loading time, and the cementitious composite's behavior relative to carbonation is separated into two loading zones. A slow increase is observed in the first zone, which varies from the undamaged condition to 2h of loading. The second zone (at 4h of loading) is characterized by a high increase in the carbonation depth due to the development of micro-cracks into the cementitious composites by a longer loading time. SCC composite with fiber shows a 20% and 52% lower carbonation depth than the SCCs composites based on limestone and siliceous aggregates, respectively. Indeed, the decrease of the porosity and the permeability with the addition of steel fiber can explain a lower residual carbonation depth.

5- Conclusion

Based on the experimental study performed on an SCC fiber composite and two other SCCs composites with limestone and siliceous aggregates, the following conclusions can be drawn:

By comparing all of the SCCs, SCC with siliceous aggregates shows a lower compressive strength in all samples. However, at 90 days, the compressive strength of the SCC composite with the fibers is found to be respectively 10% and 19% higher than the one of the SCC composite based on limestone and siliceous aggregates.

The water porosity of SCC with siliceous aggregates is higher than two other SCCs at all loading states, which shows a larger porous network from different loading in this composite.

After 90 days of aging, the SCC fibers composite showed a decrease in migration coefficient by a factor of 2.8 and 4.2, respectively, compared to the SCC composite manufactured with the limestone and siliceous aggregates. Its intrinsic permeability is lower by a factor of 1.9 and 2.2, respectively, compared to SCCs composites with limestone and siliceous aggregates. This result is related to the porous network being greater in this composite than in two other SCCs composites.

The damage of SCCs can be obtained with an applied loading state using a uniaxial compression test, up to 70% of the ultimate compressive strength (UCS). The maximum damage value increases with loading time for the three SCCs. This variation can be interpreted by the existence of microcracks and their propagation according to the applied load, as we can see from the porosimetry curves with a shift towards the larger pore diameters.

The impact of compression cracks is more pronounced on gas permeability than on diffusion coefficient. An increase of 7 for intrinsic permeability and by a factor of only 2.41 for chloride migration coefficient was obtained for the SCC composite based on siliceous aggregates with a maximum damage value of 0.214. Lower factor values were found for the SCC fibers composite, which shows the reinforcing effect of the concrete by fibers for a reduction of diffuse damage.

A linear correlation is obtained between the intrinsic permeability coefficient k_{int} and diffusion coefficient De in the damaged state, a correlation coefficient $R^2 = 0.93$. However, both do not correspond to the same transfer mechanisms.

The carbonation reaction of SCCs composites was accelerated under stressed conditions. The influence of loading time on the carbonation resistance of SCC composite-based siliceous aggregates was greater than that of two other SCCs composites. The incorporation of the steel fiber improves the carbonation resistance for structures subjected to mechanical loading.

Acknowledgments

The authors would like to thank Mr. Mehrdad Firoozan and Ms. Minoo Shahrokhi for their assistance with some laboratory measurements. The authors acknowledge the Mana Peysanjesh Consulting Engineering Laboratory for their authorization to use the apparatus.

References

[1] P. Dinakar, P.K. Sahoo, G. Sriram, Effect of metakaolin content on the properties of high strength concrete, International Journal of Concrete Structures and Materials, 7(3) (2013) 215-223.

[2] K.H. Khayat, Workability, testing, and performance of self-consolidating concrete, Materials Journal, 96(3) (1999) 346-353.

[3] D. Niknezhad, S. Kamali-Bernard, H.-A. Mesbah, Self-compacting concretes with supplementary cementitious materials: Shrinkage and cracking tendency, Journal of Materials in Civil Engineering, 29(7) (2017) 04017033.

[4] K. Samimi, S. Kamali-Bernard, A.A. Maghsoudi, M. Maghsoudi, H. Siad, Influence of pumice and zeolite on compressive strength, transport properties and resistance to chloride penetration of high strength self-compacting concretes, Construction and building materials, 151 (2017) 292-311.

[5] K. McNeil, T.H.-K. Kang, Recycled concrete aggregates: A review, International journal of concrete structures and materials, 7(1) (2013) 61-69.

[6] M. Şahmaran, Effect of flexure induced transverse crack and self-healing on chloride diffusivity of reinforced mortar, Journal of Materials Science, 42(22) (2007) 9131-9136.

[7] K. Samimi, S. Kamali-Bernard, A.A. Maghsoudi, Durability of self-compacting concrete containing pumice and zeolite against acid attack, carbonation and marine environment, Construction and building materials, 165 (2018) 247-263.

[8] D. Niknezhad, B. Raghavan, F. Bernard, S. Kamali-Bernard, Towards a realistic morphological model for the meso-scale mechanical and transport behavior of cementitious composites, Composites Part B: Engineering, 81 (2015) 72-83.

[9] K. Samimi, G.R. Dehghan Kamaragi, R. Le Roy, Microstructure, thermal analysis and chloride penetration of self-compacting concrete under different conditions, Magazine of Concrete Research, 71(3) (2019) 126-143.

[10] C. Aquino, M. Inoue, H. Miura, M. Mizuta, T. Okamoto, The effects of limestone aggregate on concrete properties, Construction and Building Materials, 24(12) (2010) 2363-2368.

[11] E. Piotrowska, Y. Malecot, Y. Ke, Experimental investigation of the effect of coarse aggregate shape and composition on concrete triaxial behavior, Mechanics of Materials, 79 (2014) 45-57.

[12] B. Raghavan, D. Niknezhad, F. Bernard, S. Kamali-Bernard, Combined meso-scale modeling and experimental investigation of the effect of mechanical damage on the transport properties of cementitious composites, Journal of Physics and Chemistry of Solids, 96 (2016) 22-37.

[13] A. Neville, Chloride attack of reinforced concrete: an overview, Materials and Structures, 28(2) (1995) 63-70.

[14] G. Chatzigeorgiou, V. Picandet, A. Khelidj, G. Pijaudier-Cabot, Coupling between progressive damage and permeability of concrete: analysis with a discrete model, International journal for numerical and analytical methods in geomechanics, 29(10) (2005) 1005-1018.

[15] H.R. Samaha, K.C. Hover, Influence of microcracking on the mass transport properties of concrete, Materials Journal, 89(4) (1992) 416-424.

[16] V. Afroughsabet, L. Biolzi, T. Ozbakkaloglu, High-performance fiber-reinforced concrete: a review, Journal of materials science, 51(14) (2016) 6517-6551.

[17] C. Lim, N. Gowripalan, V. Sirivivatnanon, Microcracking and chloride permeability of concrete under uniaxial compression, Cement and Concrete Composites, 22(5) (2000) 353-360.

[18] M. Saito, H. Ishimori, Chloride permeability of concrete under static and repeated compressive loading, Cement and Concrete Research, 25(4) (1995) 803-808.

[19] A.D. Tegguer, S. Bonnet, A. Khelidj, V. Baroghel-Bouny, Effect of uniaxial compressive loading on gas permeability and chloride diffusion coefficient of concrete and their relationship, Cement and concrete research, 52 (2013) 131-139.

[20] A. ASTM C642, Standard test method for density, absorption, and voids in hardened concrete, ASTM, ASTM International, (2013).

[21] S. Kamali-Bernard, F. Bernard, Effect of tensile cracking on diffusivity of mortar: 3D numerical modeling, Computational Materials Science, 47(1) (2009) 178-185

[22] C. Andrade, Calculation of chloride diffusion coefficients in concrete from ionic migration measurements, Cement and concrete research, 23(3) (1993) 724-742

[23] C. Andrade, C. Alonso, On-site measurements of corrosion rate of reinforcements, Construction and building materials, 15(2-3) (2001) 141-145

[24] J. Kollek, The determination of the permeability of concrete to oxygen by the Cembureau method—a recommendation, Materials and structures, 22(3) (1989) 225-230

[25] G.T. 50082-, Standard for test methods of long-term performance and durability of ordinary concrete, in, AQSIQ Beijing, China, 2009.

[26] AFPC-AFREM, Durabilité des Bétons,'Méthodes Recommandées pour la Mesure des Grandeurs Associées à la Durabilité', Compte-rendu des Journées Technique, in, Institut National des Sciences Appliquées, Université Paul Sabatier Toulouse …, 1997

[27] C. Mazzotti, M. Savoia, Nonlinear creep, Poisson's ratio, and creep-damage interaction of concrete in compression, Materials Journal, 99(5) (2002) 450-457

[28] D. Okpala, Pore structure of hardened cement paste and mortar, International Journal of cement composites and lightweight concrete, 11(4) (1989) 245-254

[29] C. Zhou, K. Li, J. Han, Characterizing the effect of compressive damage on transport properties of cracked concretes, Materials and structures, 45(3) (2012) 381-392

[30] R. Feldman, The effect of sand/cement ratio and silica fume on the microstructure of mortars, Cement and concrete research, 16(1) (1986) 31-39.

[31] J. Gonçalves, L. Tavares, R. Toledo Filho, E. Fairbairn, E. Cunha, Comparison of natural and manufactured fine aggregates in cement mortars, Cement and Concrete Research, 37(6) (2007) 924-932.

[32] X. Chen, S. Wu, Influence of water-to-cement ratio and curing period on pore structure of cement mortar, Construction and Building Materials, 38 (2013) 804-812

[33] E.J. Garboczi, Permeability, diffusivity, and microstructural parameters: a critical review, Cement and concrete research, 20(4) (1990) 591-601

[34] M.D. Lepech, V.C. Li, Water permeability of cracked cementitious composites, (2005).

[35] A. Kermani, Permeability of stressed cementitious composites, Building Research and Information, 19(6) (1991) 362-365

[36] M. Choinska, A. Khelidj, G. Chatzigeorgiou, G. Pijaudier-Cabot, Effects and interactions of temperature and stress-level related damage on permeability of concrete, Cement and Concrete Research, 37(1) (2007) 79-88

[37] T. Sugiyama, W Permeability of Stressed Cementitious Composites, C(Doctoral thesis) Dept. of Civil Engineering, (1994).

[38] A. Castel, R. François, G. Arliguie, Effect of loading on carbonation penetration in reinforced concrete elements, Cement and Concrete Research, 29(4) (1999) 561-565

[39] M.T. Liang, W.J. Qu, Y.S. Liao, A study on carbonation in concrete structures at existing cracks, Journal of the Chinese Institute of Engineers, 23(2) (2000) 143-153

[40] C.-F. Lu, Y.-S. Yuan, J.-H. Jiang, Effect of pore structure on gas diffusion in fly ash concrete, Zhongguo Kuangye Daxue Xuebao(Journal of China University of Mining & Technology), 40(4) (2011) 523-529.

[41] Y. Wang, H. Wu, V.C. Li, Concrete reinforcement with recycled fibers, Journal of materials in civil engineering, 12(4) (2000) 314-319.

HOW TO CITE THIS ARTICLE
K. Samimi, A. A. Shirzadi Javid, The durability of Self-Consolidating Concrete Containing Steel Fiber and Two Different Types of Aggregates under the Uniaxial Compression Loading , AUT J. Civil Eng., 6(2) (2022) 221-240.

DOI: 10.22060/ajce.2022.21183.5796